Auger spectroscopy of hydrogenated diamond surfaces

I. L. Krainsky and V. M. Asnin
NASA Lewis Research Center, Cleveland, Ohio 44135

A. G. Petukhov and M. Foygel
Physics Department, South Dakota School of Mines and Technology, Rapid City, South Dakota 57701-3995
(Received 31 March 1997; revised manuscript received 25 August 1997)

An energy shift and a change of the line shape of the carbon core-valence-valence Auger spectra are observed for diamond surfaces after their exposure to an electron beam, or annealing at temperatures higher then 950 °C. The effect is studied for both natural diamond crystals and chemical-vapor-deposited diamond films. A theoretical model is proposed for Auger spectra of hydrogenated diamond surfaces. The observed changes of the carbon Auger line shape are shown to be related to the redistribution of the valence-band local density of states caused by the hydrogen desorption from the surface. One-electron calculation of Auger spectra of diamond surfaces with various hydrogen coverages are presented. They are based on self-consistent wave functions and matrix elements calculated in the framework of the local-density approximation and the self-consistent linear muffin-tin orbital method with static core-hole effects taken into account. The major features of experimental spectra are explained.
[S0163-1829(97)05944-4]

I. INTRODUCTION

Auger electron spectroscopy (AES) is a powerful tool for studying the local electronic structure of solids.[1] Auger spectra incorporate very important information about materials' composition and chemical bonding. An Auger core-valence-valence process involves a three-particle interaction of two valence electrons and a core hole in the initial state and two valence holes and an Auger electron in the final state. The kinetic energy of the free Auger electron, which escapes the solid, is measured experimentally. Most of the useful information is contained in the energy distribution of these electrons. It is evident that the Auger line shape is related to both the local density of states (LDOS) of the valence band and the matrix elements of Coulomb interaction between wave functions of the initial and final states.[2]

Typical energies of the Auger electrons in diamond are within the range of 240–280 eV.[1] The mean free path of these electrons does not exceed a few interatomic distances.[1] This means that the effect of the surface density of states cannot be ignored. However, there is a perception[3] that the surface effects are not important for the interpretation of the carbon *KVV* Auger spectra. From this viewpoint, the presence of foreign atoms that are chemically bound to the surface should not affect the *KVV* Auger line shapes of the host atoms. Our recent experiments,[4] in apparent contradiction with this conclusion, have shown that the hydrogen desorption from the surface of chemical-vapor-deposited (CVD) diamond films rather significantly changes both the Auger carbon peak position (which was found to shift towards the higher energies), and its shape. These changes were attributed to a redistribution of the surface carbon valence LDOS that were dependent on the extent of hydrogen coverage of the surface.

We present the results of detailed measurements of this effect for a surface of natural single-crystal diamond. We also developed a consistent theoretical description for the above-mentioned composition trends in the *KVV* Auger spectra of hydrogenated diamond surfaces that takes into account both the surface and static core-hole effects.

In Sec. II, we will discuss experimental procedure and data on *KVV* Auger spectra of hydrogenated diamond surfaces. In Sec. III the one-electron approach to the calculations of Auger electron spectra of diamond surfaces is described. In Sec. IV the results of our theoretical analysis will be compared with the experimental data on hydrogenated surfaces of diamond. The conclusion is presented in Sec. V.

II. EXPERIMENTAL TECHNIQUE AND RESULTS

A. Sample description and preparation

The experiments were performed with both a natural single-crystal diamond and CVD diamond films.

The single-crystal sample studied was a rectangular plate, with the dimensions $4\times4\times0.3$ mm^3, and with the (111) surface. It was cut from type-IIB natural semi-insulated single-crystal diamond which is *p* type and is known to be slightly doped by boron. The sample was brazed onto a $25\times4\times1$ mm^3 sapphire strip using SnTi alloy. The back side of the strip was coated with a sputter-deposited Ti film that was used as a resistive heater. Sample temperatures of up to 1000 °C were routinely achieved in the experiments. To monitor the temperature, infrared and visual two-color pyrometers were used.

The surface of the sample was prepared employing standard technique applied for diamond.[5] It included mechanical polishing using 0.25 μm grit and olive oil followed by cleaning in ultrasonic baths with acetone and alcohol. There is a prevalent opinion that the olive oil acts as a source of hydrogen for the diamond surface.[6] The sample was mounted using platinum foil and Ta clamps on a special holder and positioned at the center of all-metal ultrahigh-vacuum cham-

ber with a base pressure of 1×10^{-10} Torr. Before the measurements, the crystal was annealed at 500 °C for 30 min to clean the surface.

CVD diamond randomly oriented polycrystalline films were grown on Mo substrates by microwave plasma CVD and were heavily doped with boron (up to 10^{20} cm^{-3}). The thickness of the films was in the range of 1–20 μm. The diamond films were not treated in any way after their deposition; nevertheless, no other elements except carbon were observed in their Auger spectra.

The decrease of hydrogen coverage of diamond surfaces was achieved by both the exposure to the beam of the cylindrical mirror analyzer (CMA) electron gun and sample annealing at temperatures higher then 950 °C.[6]

Rehydrogenation of the single-crystal diamond surface was achieved by room-temperature exposure of the diamond to atomic hydrogen, which was produced from the molecular hydrogen background by a hot tungsten filament operated at a temperature about of 1900 °C. Saturation coverage was to be observed after 30 min exposure at 1×10^{-5} Torr pressure of hydrogen. For CVD films surface, the same exposure to a molecular hydrogen environment was enough to restore hydrogen coverage.[4,7–10]

B. Measurement technique

Auger electron spectrum were measured by a single-pass (Perkin-Elmer) CMA with an energy resolution of 0.6% and collection angle of $42°\pm6°$. While the electron spectroscopy of highly doped CVD diamond films was a routine procedure, taking electron spectra of the semi-insular natural diamond crystal turned out to be a much more complicated procedure due to sample charging. To prevent charging, which usually distorts the electron spectra, we utilized a combination of the pulse method of measurements and sample heating.[11] Heating of the sample increased its conductivity and using the pulse technique prevented the charge from accumulation.

The pulsed primary current was created by applying to the Wehnelt of the CMA electron gun a sum of negative ''turn-off'' dc voltage and positive rectangular ''turn-on'' pulses from a Hewlett-Packard 8112A generator. To monitor sample charging, the secondary electron current pulses were amplified and observed on an oscilloscope. When charging of the surface occurred, we observed the pulse decaying, losing its rectangular shape and amplitude. To prevent this from happening, a proper combination of the pulse duration, frequency, sample temperature, and primary current were selected for each measurement. Our measurements have shown that at room temperature the charging occurred at a pulse duration longer than 3×10^{-7} s and frequency higher than 1 kHz at primary current density P_I ranging from 10^{-5} to 10^{-4} A/cm^{-2}. Increasing the temperature of the sample to 400–500 °C allowed us to use significantly longer pulses (up to 10^{-5} s) and higher frequency (up to 5 kHz), thereby increasing the data collecting time and the signal-to-noise ratio. The change of the pulse parameters selected for measurements by the factor of 2–4 did not affect the measured energy and shape of the Auger *KVV* line within accuracy of our instrumentation (about 0.1 eV). One of the most sensitive ways that we used to prove absence of the artifact of charging was an appropriate shift of the onset of the secondary electrons when small potentials (0.5–5 eV) are applied to the target.[10] Therefore, we concluded that the sample charging was negligible during the selected experimental procedure.

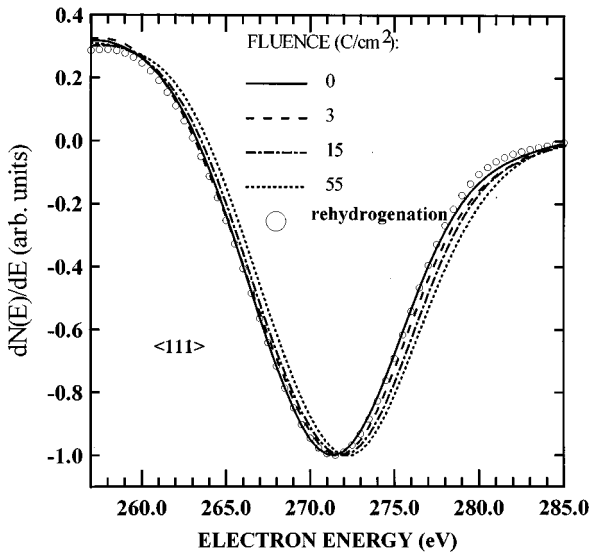

FIG. 1. Carbon A_0 Auger peak for the single-crystal diamond after various electron beam exposures (fluence range from 0 to 55 C/cm^2), and after subsequent rehydrogenation.

Current flowing along the resistive heater creates an additional unknown bias of the sample relative to the ground. To avoid this effect the sample was heated in a pulse mode and detection of the secondary electrons occurred only during the intervals between the heating current pulses. The width and the period of the heating current pulses were computer controlled and set at 1 and 2 s, correspondingly. These times were at least one order of magnitude smaller than the time required for the sample temperature to stabilize.

The data were collected under computer control by counting electron pulses from an electron multiplier, and then filtered and differentiated in order to obtain standard Auger spectra.

C. Experimental results

Figure 1 demonstrates carbon A_0 (KV_1V_1) Auger peaks for the single-crystal diamond, measured before and after exposure of the surface to the primary electron beam at various fluences (total amount of charge per unit area deposited on the surface). It can be seen that the exposure of the surface resulted in both the shift of the peak position toward higher electron energies and increase of its full width at half maximum (FWHM). Both of the changes saturated with the increase of exposure reaching the values of about 1 eV for the shift and 0.3–0.4 eV for the FWHM.

Corresponding changes of A_1 (KV_2V_2) features located at the low-energy side of the A_0 peak are shown in Fig. 2. The electron beam exposure caused the ratio of the high-energy peak amplitude to the low-energy one to decrease, as had been observed earlier.[12] All these effects were reversed almost completely after rehydrogenation of the crystal surface with atomic hydrogen. The rehydrogenation restored the Au-

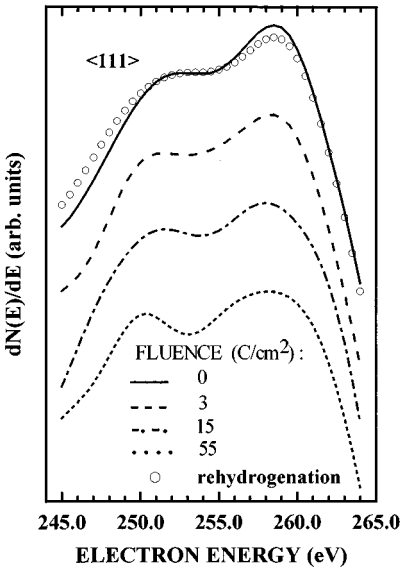

FIG. 2. Fine structure of A_1 feature for the single-crystal diamond at various electron beam exposures for the same fluences as in Fig. 1, and after subsequent rehydrogenation.

ger peak's initial position and its shape including the fine structure, as seen in Figs. 1 and 2.

The same phenomena were observed after annealing the sample at temperatures higher then 950 °C when hydrogen is well known to desorb from the diamond surface.[6] The A_0 Auger peak of the crystal surface before and after annealing are displayed in Fig. 3, where the energy shift can be clearly observed. The change of the fine structure after annealing was well documented by Pate.[6]

Exposure of the diamond surface to the primary electron beam as well as its annealing at $T \geqslant 950$ °C is well known to result in desorption of hydrogen[6,12] and a decrease of secondary yield of the CVD films.[7–10] In this study, in addition to Auger spectra of the single crystal, we were monitoring the coefficient

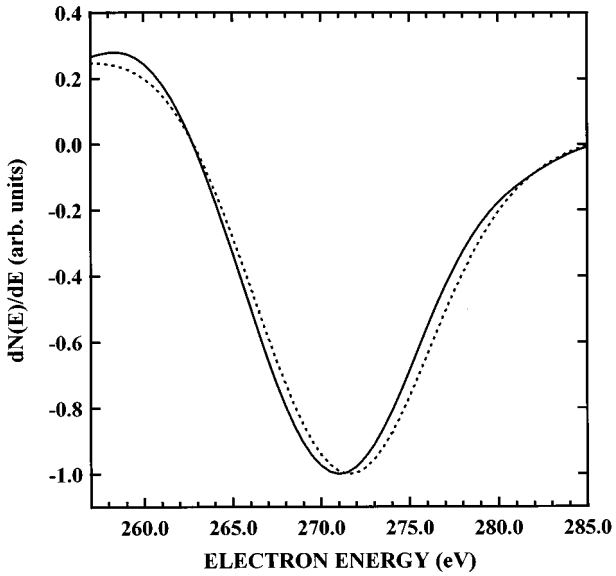

FIG. 3. Carbon A_0 Auger peak for the single-crystal diamond before (solid line) and after (dotted line) 950 °C annealing.

of the secondary electron emission σ—also in the pulse mode to avoid the charging effect. It was found that the changes of Auger spectra under the electron-beam exposure and annealing were accompanied by a sharp decrease of σ, from the initial value of 35 down to about 1. The high value of σ results from strong negative electron affinity that is specific to the hydrogen-covered diamond surface.[6,13–15] This effect reveals itself as an intense peak in the low-energy part of the spectrum of the energy distribution of the secondary electrons.[10] The peak disappeared after hydrogen was desorbed from the surface and would reappear (together with an increase of the σ value) with surface rehydrogenation.[10]

Therefore, we can conclude that observed changes in the diamond Auger spectrum were directly related to the extent of hydrogen coverage of the diamond surface.

III. COMPUTATIONAL PROCEDURE

The basic *KVV* Auger process can be described as follows. A valence-band electron is captured by a previously created core-hole state c. The energy of recombination is transferred to another nearby valence electron that now has enough energy to leave the crystal. As a result, two holes (k and l) in the valence band are generated. The energies of these holes lie in the continuous spectrum of the valence band. Therefore, the kinetic energy of the ejected Auger electron can be expressed as

$$E_A = I_c - (I_k + I_l + U_{\text{eff}}), \tag{1}$$

where $I_{c,k,l}$ are the ionization energies of the corresponding electronic states relative to the vacuum level; U_{eff} is the effective Coulomb energy of interaction between the two valence holes in the final state.[16] To calculate the energy distribution of the Auger electrons, one should integrate the probability of the elementary process over the ionization energies I_k and I_l of the valence-band holes.

A standard procedure for the calculation of the *KVV* Auger spectrum for diamond or graphite can be explained as follows.[17,18] LDOS of the valence s and p electrons, which are either evaluated theoretically or extracted from photoemission measurements, are used to calculate different convolutions of partial LDOS (s-s, s-p, and p-p) weighted with the corresponding matrix elements of Coulomb interaction. These convolutions are finally added to find the distribution of the Auger electrons. The Coulomb matrix elements are usually taken from the atomic calculations while the hole-hole partial effective interaction energies U_{eff}^{ss}, U_{eff}^{sp}, and U_{eff}^{pp} (Ref. 17) serve as fitting parameters. This procedure gives a reasonably accurate description of experimental data for graphite,[17] laser-deposited a-C, a-C:H, and single-crystal diamond.[18]

This kind of calculation usually employs a large number of parameters to fit the experimental data. Furthermore, they are usually based only on *bulk* LDOS, underestimating the influence of the surface that is expected to be very important for Auger spectra calculations, particularly with an adsorbent at the *surface*.

To analyze the effects of the hydrogen adsorption on the Auger spectra of the diamond surface we used the first-principle local-density approximation method[19] for the calculations of the LDOS and Auger matrix elements. Both the

surface and the core-hole effects were taken into account. We did not, however, introduce any fitting parameters. One would not expect that our results describe the experimental data perfectly, but they would rather give a correct semiquantitative description of the experiment.

While calculating the Auger spectrum $N(E_A)$ we adopted a simplified version of the theory of *KVV* processes developed by Almbladh and co-workers.[20] We considered the wave functions of the valence electrons involved into the basic Auger process as atomiclike linear muffin-tin orbitals (LMTO). These orbitals belong to the same atom as the core hole,[2,16,20] and therefore are perturbed by the core hole. This effect is usually referred to as a static core-hole effect.[17] Inside the crystal the wave function of the ejected Auger electron incorporates an exponentially decaying factor $\exp(-\lambda|z_j|/2)$, where $|z_j|$ is a distance of the jth atomic plane from the surface and $1/\lambda$ is a typical escape length, which in our case is of the order of 10 Å. It is possible to show then (see also Refs. 2 and 20) that

$$N(E_A)=2\pi\sum_j \exp(-\lambda|z_j|)N_j(E_A), \tag{2}$$

where

$$N_j(E_A)=\sum_{l,l'} \int_{VB} M_{ll'}(E_A-I_c,E)n_l^i(E_A-I_c-E)n_{l'}^j(E)dE. \tag{3}$$

In formulas (2) and (3) j enumerates atomic layers; $l=0,1$ (s,p) are orbital momentum quantum numbers; n_l^j are partial local densities of states, and

$$M_{ll'}=(\sqrt{2E_A}/8\pi^3)\sum_{k,l} \frac{2}{2k+1}\begin{pmatrix} l & l_c & k \\ 0 & 0 & 0 \end{pmatrix}^2 \times\begin{pmatrix} l' & l_A & k \\ 0 & 0 & 0 \end{pmatrix}^2 |R_k(l,l',l_c,l_A)|^2 \tag{4}$$

are the matrix elements of the Coulomb interaction between the wave functions of the initial and final states.

The matrix elements in Eq. (4) are expressed through Wigner $3j$ symbols and Slater radial integrals $R_k(l,l',l_c,l_A)$[21] with l_c being an orbital quantum number of the core hole (for the $1s$ carbon core state $l_c=0$); l, l', and k are the orbital quantum numbers of the valence electrons, and l_A is an orbital number of the Auger electron partial wave. In Eqs. (2) and (3) functions $N_j(E_A)$ describe contributions to the Auger spectra from the subsequent layers. The partial LDOS n_l represent the outputs of the self-consistent LMTO calculations. The matrix elements can also be calculated if the radial parts of the self-consistent LMT orbitals are known. In Eq. (4) we assume that both the wave functions of valence electrons and partial LDOS are perturbed by the $1s$ core hole localized on a carbon atom.

An eight-monolayer symmetric diamond slab was used to model a partially hydrogenated diamond surface. First-principle local-density approximation–LMTO calculations in the atomic-sphere approximation[22] were performed for the slab with (111) surface. This slab had one monolayer of hydrogen atoms on each side. Five empty spheres between periodically repeated slabs were introduced to simulate vacuum.

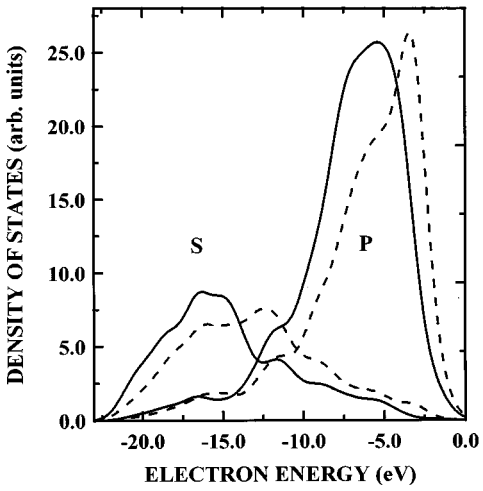

FIG. 4. s and p partial LDOS for the completely hydrogenated surface C atoms with (solid lines) and without (dashed lines) static core-hole effects taken into account.

The above-mentioned effect of the core holes on the wave functions and on the spectrum of valence electrons was taken into account by generating a two-dimensional (2D) ''superlattice'' of the $1s$ core holes localized on carbon atoms. To reduce overlapping between valence electrons surrounding different core-hole sites, the period of this ''superlattice'' was chosen to be twice as large as the period of 2D triangular lattice, representing a monolayer of carbon atoms.

We performed a series of self-consistent slab calculations of the electronic structure for different depths z_j of the core-hole layer with respect to the surface. Consequently, we calculated functions $N_j(E_A)$ with $j=1,2,3,4$, where $j=1$ corresponds to the surface layer and $j=4$ corresponds to the central (bulklike) layer.

The effect of the fractional hydrogen coverage of the (111) diamond surface was modeled by introducing a fractional effective atomic number $(0\leqslant A\leqslant 1)$ for the surface hydrogen atoms with $A=1$ corresponding to a 100% coverage, and $A=0$ corresponding to a ''clean'' unreconstructed diamond surface. Our calculations for the LDOS required integration over quasi-2D Brillouin zone. We used a mesh of 25 points in **k** space with subsequent Gaussian broadening of the obtained spectra. A half-width parameter equal to 0.08 Ry was introduced to assure sufficient smoothness of the final Auger spectra and their derivatives.

IV. DISCUSSION

Figure 4 shows the contributions of the s and p carbon states into the total LDOS for the completely hydrogenated surface with and without the static core-hole effects taken into account. It can be seen that these contributions are clearly separated in energies with the lower part of the surface valence band originated from the low-energy atomic s states and the upper band originated from the atomic p states. Taking into account the core-hole states transformed

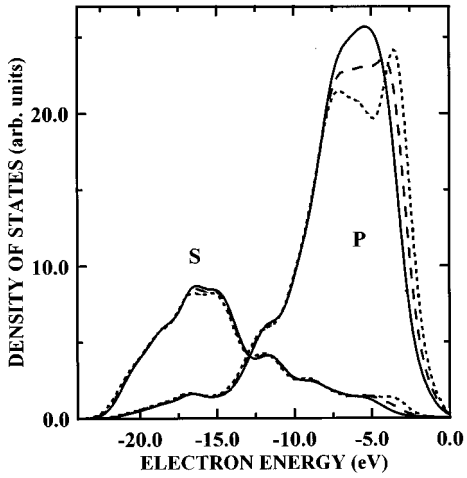

FIG. 5. *s* and *p* partial LDOS for the surface C atoms with static core-hole effects taken into account for various hydrogen coverages: 100% solid line; 80%, dashed line; 60%, dotted line.

the LDOS in two ways. It shifted both peaks toward lower energies and also broadened the *p* peak.

Our calculations showed that the C-H bond gives its main contribution to the surface LDOS in the area of the upper (*p* type) peak. Therefore, the removal of hydrogen would affect the density of states mostly in this region (Fig. 5). At coverages less than 80%, Fig. 5 displays the splitting of a separate C-H peak and its shift towards the band gap.

Figure 6 shows the contribution of the surface LDOS into the Auger spectrum of 100% hydrogen passivated (111) diamond surface. Our first-principle slab calculations confirm the fact (well-established for diamond) that the fine structure of the low-energy shoulder of the Auger spectra is determined by all the partial convolutions (*s*-*s*, *s*-*p*, and *p*-*p*) of the valence-band states. This fine structure is clearly seen in Fig. 6. It is much more pronounced for the surface contribution to the Auger spectra as compared to the bulk contribution. This is especially true for the derivative dN/dE_A of these spectra [Fig. 6(b)]. Our calculations showed that the most pronounced peak A_0 in dN/dE_A can be obviously attributed to the C-H surface states.

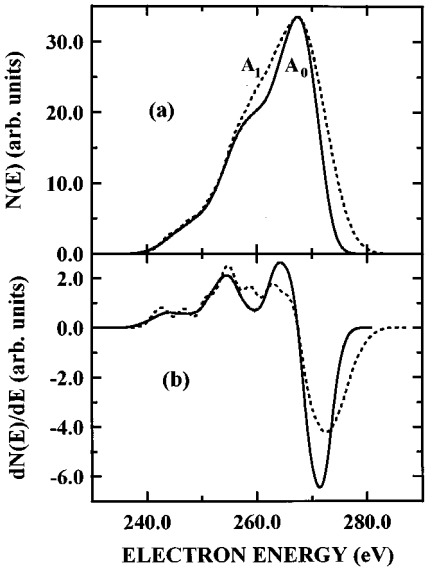

FIG. 6. Bulk (dashed lines) and surface (solid lines) contributions to the Auger spectrum (a) and its derivative (b) for 100% hydrogenated surface.

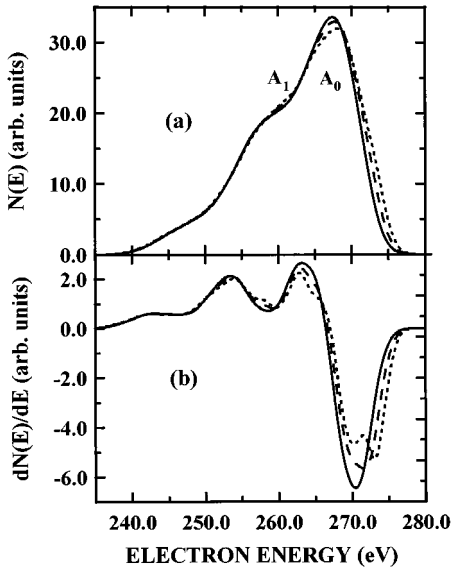

FIG. 7. Auger spectrum (a) and derivative of the Auger spectrum (b) of (111) diamond surface for various hydrogen coverages: 100%, solid line; 80%, dashed line; 60%, dotted line.

Figure 7(a) shows the effects of hydrogen coverage on the Auger spectrum of diamond. It is clearly seen that hydrogen desorption causes this spectrum to shift towards higher kinetic energies and to broaden slightly. These effects are due to changes of partial LDOS for the *p* states as it is displayed in Fig. 5.

The changes in the derivatives of the Auger spectra calculated for different hydrogen coverages appear to be more obvious [Fig. 7(b)]. The removal of hydrogen has the strongest influence on both the position and the shape of the main minimum, as we just discussed. It also can be seen that the low-energy fine structure is affected.

The results of the calculations are in qualitative agreement with the observed behavior of the carbon Auger peak during hydrogen desorption from the diamond surface. Comparison of the experimental data from Figs. 1–3, and Ref. 4 (for the CVD diamond films) with the theoretical calculations from Fig. 7 shows that the calculations give the right description of the high-energy shift and broadening of Auger peak while their measured values are smaller than the theoretical predictions. It can also be concluded from these figures that the tendencies in the fine-structure change are correctly described by our theoretical model. It is necessary to note, however, that our calculations did not take into account the surface lattice reconstruction that occurs at small hydrogen coverage of the diamond surface.[6] This reconstruction was shown to result in the appearance of a DOS peak at 1.1 eV below the top of the valence band[6] that can apparently limit the value of the Auger peak shift and the change of its width. The neglect of the surface reconstruction might also be responsible for the appearance of the artificial splitting of the

A_0 peak in the theoretical Auger spectrum (Fig. 7) that has not been observed experimentally.

V. CONCLUSION

We have shown that the energy of the carbon Auger peak and its shape for the diamond surface are indeed sensitive to the extent of hydrogen coverage of the surface. We have observed the shift of the AES carbon peak towards higher energies together with increase of its FWHM for both the single-crystal diamond and polycrystalline CVD diamond films while the hydrogen coverage was reduced as the result of electron beam exposure or the sample annealing.

The theoretical model of Auger spectra of hydrogenated diamond surfaces has been developed. We have shown that the experimentally observed changes in carbon Auger line shape can be related to the redistribution of the valence-band local density of states caused by the hydrogen desorption from the surface. One-electron calculations of Auger spectra of the diamond (111) surface with various hydrogen coverages were performed. They were based on self-consistent wave functions and matrix elements calculated in the framework of the local-density approximation and the self-consistent linear muffin-tin orbital method with static core-hole effects taken into account. The major features of the experimental spectra have been qualitatively explained.

ACKNOWLEDGMENTS

The authors appreciate S. V. Pepper for providing us with the single-crystal diamond used in the experiments. This work was supported by NASA Grant No. NAG 3-1680 and the National Research Council. One of us (A.G.P.) acknowledges financial support and the hospitality of the NASA Summer Faculty Fellowship Program.

[1] P. Weightman, Rep. Prog. Phys. **45**, 753 (1982).
[2] P. J. Fibelman, E. J. McGuire, and K. C. Pandey, Phys. Rev. Lett. **36**, 1154 (1976); Phys. Rev. B **15**, 2202 (1977); P. J. Fibelman and E. J. McGuire, Phys. Rev. B **17**, 690 (1978).
[3] D. R. Jennison, Phys. Rev. B **18**, 6865 (1978).
[4] I. L. Krainsky, G. T. Mearini, V. M. Asnin, H. Sun, M. Foygel, and A. G. Petukhov, Appl. Phys. Lett. **68**, 2017 (1996).
[5] J. Wilk and E. Wilk, *Properties and Applications of Diamond* (Butterworth, Heinmann, 1991), Chap. 9.
[6] B. B. Pate, Surf. Sci. **165**, 83 (1986).
[7] G. T. Mearini, I. L. Krainsky, and J. A. Dayton, Jr., Surf. Interface Anal. **21**, 138 (1994).
[8] G. T. Mearini, I. L. Krainsky, Y. X. Wang, J. A. Dayton, Jr., R. Ramasham, and M. F. Rose, Thin Solid Films **253**, 151 (1994).
[9] G. T. Mearini, I. L. Krainsky, J. A. Dayton, Yaxin Wang, Christian Zorman, John C. Angus, and R. W. Hoffman, Appl. Phys. Lett. **65**, 2702 (1994).
[10] I. L. Krainsky, V. M. Asnin, G. T. Mearini, and J. A. Dayton, Jr., Phys. Rev. B **53**, R7650 (1996).
[11] I. M. Bronshtein and B. S. Freiman, *Secondary Electron Emission* (Nauka, Moscow, 1969) (in Russian).
[12] S. V. Pepper, Appl. Phys. Lett. **38**, 344 (1981).
[13] F. J. Himpsel, J. A. Knapp, J. A. van Vechten, and D. E. Eastman, Phys. Rev. B **20**, 624 (1979).
[14] B. B. Pate, W. E. Spicer, T. Ohta, and I. Lindau, J. Vac. Sci. Technol. **17**, 1087 (1980).
[15] C. Bandis and B. B. Pate, Phys. Rev. B **52**, 12 056 (1995).
[16] M. Cini, Solid State Commun. **24**, 681 (1977); J. Phys. Condens. Matter **1**, SB55 (1989).
[17] J. E. Houston, J. W. Rogers, Jr., R. R. Rye, F. L. Hutson, and D. E. Ramaker Phys. Rev. B **34**, 1215 (1986).
[18] P. Kovarik, E. B. D. Bourdon, and R. H. Prince, J. Vac. Sci. Technol. A **12**, 1496 (1994).
[19] P. Hohenberg and W. Kohn, Phys. Rev. **136**, B864 (1964); W. Kohn and L. J. Sham, *ibid.* **140**, A1133 (1965).
[20] C.-O. Almbladh, A. L. Morales, and G. Grossmann, Phys. Rev. B **39**, 3489 (1989); C.-O. Almbladh and A. L. Morales, *ibid.* **39**, 3503 (1989).
[21] J. C. Slater, *The Self-Consistent Field for Molecules and Solids* (McGraw-Hill, New York, 1974), Vol. 4, p. 35.
[22] O. K. Andersen, O. Jepsen, and M. Sob, in *Electronic Band Structure and its Applications*, edited by M. Yussouff (Springer, Heidelberg, 1987), p. 1.